Optical properties of a spherical electron gas in the presence of a uniform magnetic field

A. Goker , P. Nordlander

Department of Physics and Department of Electrical and Computer Engineering
Rice Quantum Institute
M.S. 61, Rice University
Houston, TX 77251-1892, USA

ABSTRACT

We calculate the plasmon frequencies of an electron gas on a two-dimensional spherical surface within the framework of RPA (random phase approximation) when a weak uniform magnetic field is applied on the sphere. We show that a coupling between different angular momentum numbers in the excitation process takes place due to the existence of the magnetic field. We investigate how the plasmon energies vary as a function of the density of electrons on the sphere with and without the magnetic field. We also show that an electron Wigner lattice on a two-dimensional spherical surface can be regarded as a nanoshell with infinitesimal thickness by comparing the plasmon dispersion relation in former case with the semiclassical equation for nanoshells in zero magnetic field. Further issues regarding the finite thickness are discussed.

Keywords: Zeeman, Lindhard, RPA, Magnetoplasmon, Nanophotonics

1. INTRODUCTION

Recently, there has been growing interest in charged particles confined to a three-dimensional surface with a uniform magnetic field applied along one of the symmetry axes. The motion of electrons under a constant magnetic field on a sphere has been initially considered by Haldane,[1] and others[2–4] to investigate the fascinating phenomenon of fractional quantum Hall effect. This model has also proved to be useful to calculate the properties of a system of N independent particles.

In recent years, it has been possible to manufacture spherical shaped nanostructures ranging from fullerene size to nanosized objects such as SiO_2 balls in opals,[5] nanoshells[6] and multielectron bubbles.[7,8] The motion of charged particles on such spheres with constant magnetic field along a given axis of the sphere has been studied previously.[9–12] The energy spectrum was calculated and the thermodynamical properties, such as magnetization and susceptibility, were studied rigorously.

In the case of multielectron bubbles, the electrons move freely in the direction tangential to the spherical helium surface, therefore they effectively form a spherical two-dimensional electron gas. S2DEG's can also be realized in charge droplets[13] and in doped semiconductor particles if carriers accumulate in a surface layer.[14] Previously, many-body properties of such a system were investigated within the random-phase approximation scheme, where multipole excitation modes with angular momentum $l = 1, 2, 3, 4$ of the S2DEG have been calculated[15] and the angular-momentum dependent dielectric function of the S2DEG has been derived[16] Also, an exact solution for this system in weak and strong magnetic fields was developed.[17]

Motivated by these recent works, we will analyze S2DEG by using RPA formalism when the sphere is subjected to a weak uniform magnetic field along a given axis. In this regime, we can treat the system perturbatively and the magnetic field helps to achieve Zeeman effect where the degeneracy is lifted as the electronic energy levels shift due to the applied magnetic field. We investigate how the dipolar plasmon energy is affected as the magnetic field is swept or the density of electrons is changed. We hope to provide insight as to how these magnetoplasmons can be useful in developing successful nanophotonics applications.

Further author information: (Send correspondence to P.N.)
P.N.: E-mail: nordland@rice.edu, Telephone: 1 713 348 5171
A.G.: E-mail: agoker@rice.edu, Telephone: 1 713 348 3541

2. THEORY

In this section, we will develop the theoretical framework within which we treated the S2DEG. We will first describe the novelty the perturbation due to the weak magnetic field brings into the ground state of the electron gas. We will then use this result to obtain the response properties of the S2DEG by using linear response theory in second quantization.

We would like to first study the motion of electrons on a sphere of radius r_0 in Landau gauge. Throughout this paper, we will assume closed shell configuration for the ground state of the electron gas, i.e. all the angular momentum states, until the fermi level are fully occupied with two projections of spin and excitations to the fermi level are not allowed, therefore defining the Fermi angular momentum number L_F completely determines the number of electrons in the system by

$$N = 2(L_F + 1)^2 \tag{1}$$

and the areal density is

$$\nu = N/(4\pi r_0^2). \tag{2}$$

We will use a confining potential of the form

$$V(r) = \begin{cases} 0 & \text{for } r_0 < r < r_0 + \delta r \\ \infty & \text{otherwise} \end{cases} \tag{3}$$

in the Schrodinger equation. If we assume $\delta r \ll r_0$, this potential describes a shell with infinitesimal thickness, thus the radial and angular variables of the Schrodinger equation can be separated. If the fermi level lies below the first excited level of the radial component of the wave function, we can ignore the radial component and put $r = r_0$ in the remaining angular part of the hamiltonian H_Ω. This requires $\delta r \leq \nu^{-1/2}$ and, if satisfied, means that we are dealing with an effectively two-dimensional system. Now, we apply a uniform magnetic field along z axis of the sphere ($\theta = 0$). Since the system has rotational symmetry, an eigenfunction can be written as $\Psi(\theta, \phi) = \Theta(\theta)\exp(im\phi)$ in the spherical coordinates, where $m\hbar$ is the eigenvalue of $\hat{L}_z$. The angular part of the Schrodinger equation in atomic units takes the form

$$\frac{\partial}{\partial\zeta}(1-\zeta^2)\frac{\partial\Theta}{\partial\zeta} + [\varepsilon - 2mp - \frac{m^2}{1-\zeta^2} - p^2(1-\zeta^2)]\Theta = 0 \tag{4}$$

upon introducing $\zeta = \cos\theta$, the dimensionless energy $\varepsilon = 2r_0^2 E$ and the number of flux quanta p encircled by the sphere which is given by

$$p = \frac{\pi B r_0^2}{\Phi_0} \tag{5}$$

where $\Phi_0 = \frac{2\pi}{e} = 2 \times 10^{-15} Tm^2$ is the flux quantum.

Above equation is well-known and called spheroidal differential equation. Its properties were investigated by many sources.[18,19] In the absence of magnetic field, this equation reduces to the standard free rotator problem in quantum mechanics and the wave functions are the spherical harmonics. In the presence of weak magnetic field, however, one is able to develop perturbation theory around initial wave functions as long as $p^2 \leq 4l$[17] to get a series of Zeeman-split $(2l+1)$ states with energy eigenvalues

$$\varepsilon_{lm}(p) = l(l+1) + 2pm + \frac{p^2}{2}[1 + \frac{m^2}{l^2}] + \frac{p^2}{l} \tag{6}$$

and the normalized wave functions

$$\Psi_{lm}(p,\Omega) = \frac{Y_{lm}(p,\Omega) + \frac{p^2}{l}Y_{l+2,m}(p,\Omega) + \frac{p^2}{l}Y_{l-2,m}(p,\Omega)}{\sqrt{1 + \frac{2p^4}{l^2}}}, \tag{7}$$

where Ω denotes the spherical angles $\Omega = \{\theta, \phi\}$ and (l, m) represent the angular momentum state.

Our aim in this paper is to use the above perturbed energy eigenvalues and wavefunctions to develop a many-body description of the S2DEG in the random phase approximation (RPA) framework and, in particular,

to investigate the behaviour of the dipolar plasmon energy in presence of the magnetic field since the light excites only this plasmon mode. We will start by expressing in second quantization the surface density on the sphere which is the expectation value of the number of electrons in an infinitesimal spherical angle around Ω as

$$\hat{n_e}(p,\Omega) = \sum_{l=0}^{\infty}\sum_{m=-l}^{l}\sum_{l'=0}^{\infty}\sum_{m'=-l'}^{l'} \Psi^*_{l,m}(p,\Omega)\Psi_{l',m'}(p,\Omega)\hat{c}^\dagger_{l,m}\hat{c}_{l',m'}, \tag{8}$$

where $\Psi_{l',m'}(p,\Omega)$ refers to eq. (7). $\hat{c}^\dagger_{l,m}$ is the fermion creation operator which creates an electron in the state $\Psi_{l,m}(p,\Omega)$ on the sphere if no electron is present in that state and $\hat{c}_{l,m}$ is the fermion destruction operator which destroys an existing electron in the single particle state $\Psi_{l,m}(p,\Omega)$. We will not be considering the spin orientation of the electrons in our notation explicitly, since the total number of electrons is simply twice as much as the number of electrons with one spin orientation, thus it suffices to do the computation for the latter case. Spin orientation will come into play only when we compute the density of electrons later on.

We can also expand the density operator $\hat{n}_e(p,\Omega)$ in spherical harmonics which is a complete orthonormal set as

$$\hat{n}_e(p,\Omega) = \sum_{l=0}^{\infty}\sum_{m=-l}^{l}\hat{\rho}_e(l,m)Y^*_{lm}(\Omega). \tag{9}$$

If we invert this equation by using the orthogonality relation of the spherical harmonics and insert eq.(8) for $\hat{n}_e(p,\Omega)$, we obtain the the spherical components of the density operator as

$$\hat{\rho}_e(p,l,m) = \sum_{L=0}^{\infty}\sum_{M=-L}^{L}\sum_{l'=0}^{\infty}\sum_{m'=-l'}^{l'}[\int Y_{lm}(\Omega)\Psi^*_{L,M}(p,\Omega)\Psi_{l',m'}(p,\Omega)\,d\Omega]\hat{c}^\dagger_{L,M}\hat{c}_{l',m'}, \tag{10}$$

where (l',m') and (L,M) denote the initial and final angular momentum states respectively. (l,m) is the excitation connecting these two.

The interaction of the electrons moving on the surface of the sphere is entirely described by the Coulomb potential energy in the Hamiltonian and this term is unaffected by the presence of the magnetic field. In second quantization, it is given by

$$\hat{H}_{Coulomb} = \sum_{l_1,m_1}\sum_{l_2,m_2}\sum_{l,m}(-1)^m v(l) \times \hat{c}^\dagger_{(l_1,m_1)\otimes(l,-m)}\hat{c}^\dagger_{(l_2,m_2)\otimes(l,m)}\hat{c}_{l_2,m_2}\hat{c}_{l_1,m_1}, \tag{11}$$

where $v(l,r_0) = \frac{1}{2r_0(2l+1)}$ is the interaction amplitude and the operator $\hat{c}^\dagger_{(l_1,m_1)\otimes(l,-m)}$ creates an electron in a state which results from the combination of two states with (l_1,m_1) and $(l,-m)$.[16] Intuitively, the Coulomb interaction term represents the exchange of a virtual photon with (l,m) between two electrons in initial states with (l_1,m_1) and (l_2,m_2).

In linear response theory, an induced electron density $\rho_{ind}(p,\Omega,\omega)$ is generated when an external field $V_{ext}(\Omega,\omega)$ which couples to the electron density is applied. Its spherical components can be written as

$$\rho_{ind}(p,l,m,\omega) = V_{ext}(l,m,\omega)D_R(p,l,m,\omega), \tag{12}$$

where $D_R(p,l,m,\omega)$ is the retarded density-density Green's function. It is derived from the density-density Green's function:

$$D(p,l,m,t) = i < \Psi_0|\tau\hat{\rho}_e(p,l,m,t)\hat{\rho}_e(p,l,-m,t)|\Psi_0 >, \tag{13}$$

where τ is the time ordering operator, expectation value is taken with respect to the many body ground state and the interaction picture is used in spherical components of the density operator to bring in time dependence. We can now obtain the Lindhard or independent electron response function $D^0_R(p,l,m,\omega)$ easily by replacing

the wavenumber with the angular momenta in standard Green's function techniques. After making use of the analytical continuation, it turns out to be

$$D_R^0(r_0,p,l,m,\omega) = \sum_{l',m'}\sum_{L,M} n(l',m')(1-n(L,M))\Big|\int Y_{l,m}(\Omega)\Psi^*_{L,M}(p,\Omega)\Psi_{l',m'}(p,\Omega)\,d\Omega\Big|^2 \times\Big(\frac{1}{\omega+E_{l',m'}(r_0,p)-E_{L,M}(r_0,p)+i\eta}-\frac{1}{\omega+E_{L,M}(r_0,p)-E_{l',m'}(r_0,p)+i\eta}\Big). \quad (14)$$

In this expression, $n(l',m')$ and $n(L,M)$ denote the occupancy of the initial and final angular momentum states respectively and (l,m) represents the excitation. η is an infinitesimal number and $2r_0^2E_{l',m'}$ is given by eq. (6).

As for the integral in this expression, we will write $\Psi_{p,l'}(\Omega)$ and $\Psi^*_{p,L}(\Omega)$ explicitly by using eq. (7) and ignore the higher order terms involving p^4 in the resulting integrand. This allows us to write the integral with five terms as

$$\begin{aligned}\int Y_{lm}(\Omega)\Psi^*_{L,M}(p,\Omega)\Psi_{l',m'}(p,\Omega)\,d\Omega &= (1+\frac{2p^4}{l'^2})^{-1/2}(1+\frac{2p^4}{L^2})^{-1/2}\times\Big(\int Y_{lm}(\Omega)Y^*_{L,M}(\Omega)Y_{l',m'}(\Omega)\,d\Omega\\ &+\int Y_{lm}(\Omega)Y^*_{L,M}(\Omega)\frac{p^2}{l'}Y_{l'+2,m'}(\Omega)\,d\Omega+\int Y_{lm}(\Omega)Y^*_{L,M}(\Omega)\frac{p^2}{l'}Y_{l'-2,m'}(\Omega)\,d\Omega\\ &+\int Y_{lm}(\Omega)\frac{p^2}{L}Y^*_{L+2,M}(\Omega)Y_{l',m'}(\Omega)\,d\Omega+\int Y_{lm}(\Omega)\frac{p^2}{L}Y^*_{L-2,M}(\Omega)Y_{l',m'}(\Omega)\,d\Omega\Big). \quad (15)\end{aligned}$$

We will use the following identity[20] to evaluate the integral of three spherical harmonics

$$\int Y^*_{LM}(\Omega)Y_{l,m}(\Omega)Y_{l',m'}(\Omega)\,d\Omega=\sqrt{\frac{(2l+1)(2l'+1)}{4\pi(2L+1)}}<ll';00|ll';L0><ll';mm'|ll';LM>. \quad (16)$$

We can now take the square of the five term expression in absolute value. All the cross-terms would vanish due to the orthogonality of the Clebsch-Gordon coefficients therefore we end up with squaring the initial five terms. In the next step, we will use the below definition[21] to convert the Clebsch-Gordon coefficients to Wigner 3j-symbols

$$\begin{pmatrix} l & l' & L\\ m & m' & -M\end{pmatrix}=(-1)^{l-l'+M}(2L+1)^{-1/2}<ll';mm'|ll';LM>, \quad (17)$$

where the parenthesized (2×3) array of numbers in eq. (17) is the Wigner 3j-symbol. This prescribes which electronic transition processes contribute to excitations of the electron gas. The value of this symbol vanishes unless $|L-l'|\le l\le L+l'$ and L+l+l'=even integer. In the nonvanishing case, if we set l+l'+L=2k (k=integer), the value of the squared 3j-symbol is explicitly given by

$$\begin{pmatrix} l & l' & L\\ 0 & 0 & 0\end{pmatrix}^2=\frac{(l'+L-l)!(L+l-l')!(l+l'-L)!}{(l'+L+l+1)!}\times\Big(\frac{p!}{(p-l')!(p-L)!(p-l)!}\Big)^2 \quad (18)$$

The next task is to carry out the summations over m' and M in the Lindhard term. This is nontrivial since both the second Clebsch-Gordon coefficient and the perturbed energy eigenvalues are m' and M dependent. This necessitates a valid approximation. We will use $m'=l'$ and $M=l'+1$ in the perturbed energy eigenvalues and carry out the summations over m' and M only for the Clebsch-Gordon coefficient using the identity

$$\sum_{m'=-l'}^{l'}\sum_{M=-L'}^{L'}\begin{pmatrix} l_1 & l' & L\\ m_1 & m' & -M\end{pmatrix}\begin{pmatrix} l_2 & l' & L\\ m_2 & m' & -M\end{pmatrix}=\frac{1}{2l_1+1}\delta_{l_1,l_2}\delta_{m_1,m_2}. \quad (19)$$

This seemingly contradictory approximation is justified in two ways. First, it is consistent with dipole transition rules. Second, even if one prefers to choose a different initial magnetic quantum number, since the energy term has $1/r_0^2$ prefactor which is on the order of 10^{-6} for the typical radii in atomic units, it would hardly change the

precision of the resulting plasmon energies unless fermi level is very high. We will be avoiding that regime in this paper. In essence, this approximation means that we are carrying out the summations in the regime where the difference in energy eigenvalues is quite insensitive to the magnetic quantum number dependence. Hence, according to this approximation, the energy difference $\triangle E_{L,l'}(r_0,p) = E_{L,l'+1} - E_{l',l'}$, is given by

$$\triangle E_{L,l'}(r_0,p) = \frac{1}{2r_0^2}(L(L+1) - l'(l'+1) + 2p + \frac{p^2}{2}(\frac{(l'+1)^2}{L^2} - 1) + p^2(\frac{1}{L} - \frac{1}{l'})). \tag{20}$$

After handling the magnetic quantum number dependent Clebsch-Gordon coefficient this way and converting the other one to Wigner 3j-symbol, the final expression for the magnetic field dependent Lindhard response function becomes

$$\begin{aligned} D_R^0(r_0,p,l,\omega) &= \sum_{l'}\sum_{L} n(l')(1-n(L))\frac{1}{4\pi}\frac{1}{1+2p^4/l'^2}\frac{1}{1+2p^4/L^2} \times ((2l'+1)(2L+1)\begin{pmatrix} l & l' & L \\ 0 & 0 & 0 \end{pmatrix}^2 \\ &+(2l'+1)(2L+5)\begin{pmatrix} l & l' & L+2 \\ 0 & 0 & 0 \end{pmatrix}^2 \frac{p^4}{L^2} + (2l'-3)(2L+1)\begin{pmatrix} l & l'-2 & L \\ 0 & 0 & 0 \end{pmatrix}^2 \frac{p^4}{l'^2} \\ &+(2l'+5)(2L+1)\begin{pmatrix} l & l'+2 & L \\ 0 & 0 & 0 \end{pmatrix}^2 \frac{p^4}{l'^2} + (2l'+1)(2L-3)\begin{pmatrix} l & l' & L-2 \\ 0 & 0 & 0 \end{pmatrix}^2 \frac{p^4}{L^2}) \\ &\times(\frac{1}{\omega - \triangle E_{L,l'}(r_0,p) + i\eta} - \frac{1}{\omega + \triangle E_{L,l'}(r_0,p) + i\eta}). \end{aligned} \tag{21}$$

The reason why we preferred to write the final expression in terms of Wigner 3j-symbols rather than Clebsch-Gordon coefficients is that they illuminate more clearly which terms are allowed in the summation for the Lindhard response function. This will be very crucial for the analysis in the next section. The calculation of the RPA dielectric function can be accomplished in a straightforward manner by using a Dyson series once we know the Lindhard response function given by eq. (21). RPA dielectric function turns out to be

$$\epsilon_{RPA}(r_0,p,l,\omega) = 1 - v(l,r_0)D_R^0(r_0,p,l,\omega). \tag{22}$$

3. RESULTS AND DISCUSSION

In many-body theory of the two-dimensional homogeneous spherical electron gas, two types of excitations are possible: single particle excitations and surface plasmons. In first case, the imparted angular momentum is absorbed completely by a single electron and it gets excited to a higher angular momentum state. On the other hand, surface plasmons are waves that propagate along the surface of a conductor, usually a metal. In essence, these are light waves that are trapped on the surface because of their interaction with the free electrons of the conductor. The free electrons respond collectively by oscillating in resonance with the light wave, and this resonant interaction between the surface charge oscillation and the electromagnetic field of the light forms the surface plasmon. In both single-particle excitations and the surface plasmons, the excitation is characterized by the angular momentum l and energy ω.

Surface plasmon energies appear when the dielectric function defined by eq. (22) satisfies the following two equations:

$$Im[\epsilon_{RPA}(r_0,p,l,\omega)] = 0 \tag{23}$$

$$Re[\epsilon_{RPA}(r_0,p,l,\omega)] = 0. \tag{24}$$

Now, the first equation brings the only condition that $\omega \neq \triangle E_{L,l'}(r_0,p)$ which means the plasmon energies lie outside the region of single-particle excitations defined by $\omega = \triangle E_{L,l'}(r_0,p)$. In order to find the values of plasmon energies, one has to solve eq. (24) for successive values of l. Throughout the rest of the paper, we will concentrate on the dipolar plasmon energy since light excites only this mode. This means we have to solve eq. (24) for $l = 1$ therefore it is crucial to determine the range in which we should carry out five different summations over initial state l' and final state L in eq. (21) for all five terms that involve different Wigner 3j-symbols. We need to include only those terms for which Wigner 3j-symbol is not zero in each case.

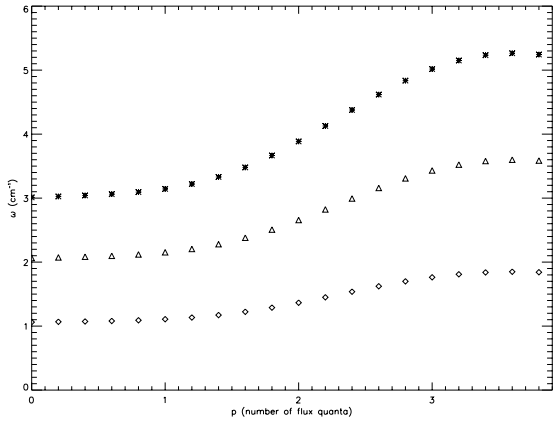

Figure 1. This figure shows the dependence of dipolar plasmon energy on the magnetic field for a sphere of 882 electrons. X-axis shows p, the number of flux quanta piercing through the sphere. The radius is 3980 a.u. for stars, 5117 a.u. for triangles and 7960 a.u. for diamonds.

We can now start considering each Wigner 3j-symbol separately. The first term which involves $\begin{pmatrix} l & l' & L \\ 0 & 0 & 0 \end{pmatrix}^2$ is the only term that survives in zero magnetic field limit where other four terms with p dependence vanish. This Wigner symbol is zero unless $|L-l'| \leq 1 \leq L+l'$ which implies l' summation for this term runs from L_F-1 to L_F while L summation runs from l' to $l'+1$. Obviously, the only allowed excitation here is from L_F to L_F+1. Next two terms involve $\begin{pmatrix} l & l' & L+2 \\ 0 & 0 & 0 \end{pmatrix}^2$ and $\begin{pmatrix} l & l'-2 & L \\ 0 & 0 & 0 \end{pmatrix}^2$. They vanish unless $|L+2-l'| \leq 1 \leq L+l'+2$ and $|L-l'+2| \leq 1 \leq L+l'-2$ respectively. These inequalities can never be satisfied since final angular momentum state L is always greater than initial one l', hence there is no allowed excitation for these two terms. They do not contribute at all in summations over initial and final angular momentum states.

Finally, let us consider the remaining two terms, namely those two that involve $\begin{pmatrix} l & l'+2 & L \\ 0 & 0 & 0 \end{pmatrix}^2$ and $\begin{pmatrix} l & l' & L-2 \\ 0 & 0 & 0 \end{pmatrix}^2$. They vanish unless $|L-l'-2| \leq 1 \leq L+l'+2$ and $|L-l'-2| \leq 1 \leq L+l'-2$ respectively. This means that summation over l' for these terms runs from L_F-3 to L_F while summation over L runs from l' to $l'+3$. For example, an excitation from L_F to L_F+3 is allowed for these terms even though we are exciting the sphere with an $l=1$ mode. This is a very remarkable consequence and the mechanism behind this apparent coupling between $l=1$ and $l=3$ modes is the presence of the magnetic field. When we turn off the magnetic field, $p=0$ and these two extra terms vanish so $l=1$ and $l=3$ modes decouple again. Magnetic field mediates the coupling between these two plasmon modes through p^4 term at the end of these two terms.

In figures 1 and 2 we plotted the dipolar plasmon energy as a function of the number of flux quanta piercing through the sphere for three different radii to demonstrate this coupling effect. In figure 1, the Fermi angular momentum number is 20 therefore the number of electrons is 882 since we assume closed-shell configuration. As soon as we turn on the magnetic field, dipolar plasmon energy starts increasing from its zero-field value which is just the $l=1$ plasmon. In non-zero magnetic field regime, $p \neq 0$ anymore therefore $l=1$ and $l=3$ modes start coupling and the value of the dipolar plasmon mode is somewhere between the zero-field values of these two, in other words both of these modes have a weight in the non-zero field value and as the strenghth of the field increases, so does the weight of the $l=3$ mode and that is the reason behind the increasing blue-shift in dipolar plasmon mode as a function of the magnetic field. We should also point out that we achieve more blue-shift for

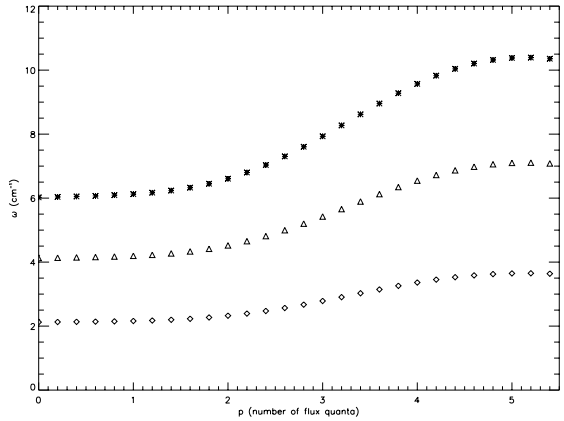

Figure 2. This figure is complimentary to fig. 1 and shows the plasmon energy as a function of the number of flux quanta piercing through the sphere. Again, the radius is 3980 a.u. for stars, 5117 a.u. for triangles and 7960 a.u. for diamonds. In this case, however, number of electrons is 3528 so surface electron densities are 4 times larger than those in fig. 1.

same number of flux quanta for smaller spheres in these figures. This is simply because we need higher magnetic fields to obtain the same number of flux quanta as the radius gets smaller which can be easily understood from eq. (5). For example, $p = 3$ corresponds to a magnetic field of 4.33×10^{-2}T for a sphere of 3980 a.u. whereas, for a sphere of radius 7960 a.u, this reduces to 1.08×10^{-2}T due to quadratic dependence on radius.

Fig. 2 illustrates the effect of changing the number of electrons on the sphere while keeping the radius constant. In this figure, the Fermi angular momentum number is 41 therefore the number of electrons is 3528. The radii are the same as the ones we used in fig. 1 hence surface electron densities are 4 times larger. Zero-field plasmon energies for all radii almost double compared to figure 1 due to the linear dependence on Fermi angular momentum number in the Lindhard response function. In essence, these figures reveal that the function of changing radius while keeping the number of electrons constant is to shift the whole curve up or down and to reduce or increase the maximum blue-shift achieved.

The last point we have to touch upon about these figures is the strength of the magnetic field after which this perturbative approach fails. We should recall the perturbed wavefunction eq. (7) in order to understand this. Since all excitations take place around L_F, l appearing in this wavefunction take values close to L_F while carrying out the summation in the Lindhard response function. This means when p^2 starts approaching L_F, second and third terms in the perturbed wavefunction become comparable to the first one due to $\frac{p^2}{l}$ factor preceeding them. Our current perturbative treatment fails thereafter obviously. For this reason, we plotted our figures up until dipolar plasmon energy saturated. This corresponds to $p = 3.6$ in fig. 1 where $L_F = 20$ and $p = 5.2$ in fig. 2 where $L_F = 41$. Our present treatment is valid only until these p values.

Next, we will investigate the behaviour of the dipolar plasmon energy as a function of the number of electrons for constant radius and try to demonstrate the nature of the mixing between different modes explicitly in weak magnetic field. In fig. 3 we plotted the $l = 1$ and $l = 3$ plasmon energies in zero magnetic field for a sphere of radius 3980 a.u. alongside with the dipolar plasmon energy when a uniform magnetic field of 0.029T is applied. Dipolar plasmon energy consists of the admixture of $l = 1$ and $l = 3$ modes and as the number of electrons increases the weight of the $l = 3$ mode decreases as seen from the figure. We can explain the reason of this by considering eq. (21). The contribution of the $l = 3$ mode is contained only in the last two terms in this expression as we discussed before. Increasing the number of electrons on the sphere means increasing the Fermi angular momentum number L_F. This clearly implies initial and final angular momentum numbers l' and L also start increasing since they are close to L_F, however we keep magnetic field constant so p is constant too. Hence $\frac{p^4}{L^2}$

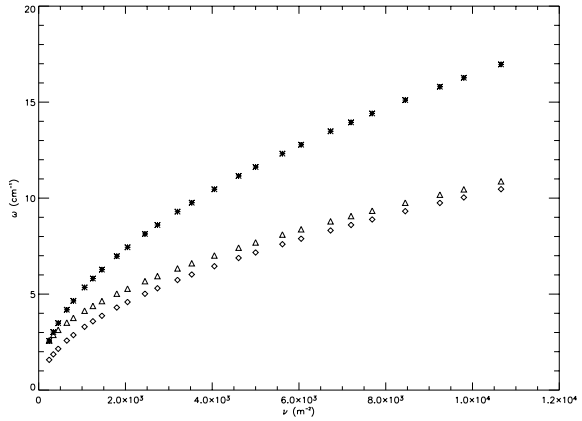

Figure 3. This figure demonstrates the dependence of the dipolar plasmon energy on the number of electrons on the sphere. The radius is constant and 3980 a.u. Diamonds and stars denote the plasmon energies for $l = 1$ and $l = 3$ modes respectively in zero magnetic field. Triangles represent the dipolar plasmon energies when a magnetic field of 0.029T is applied on the sphere.

and $\frac{p^4}{l'^2}$ factors in the last two terms in eq. (21) start decreasing as we increase the number of electrons and this reduces the weight of the $l = 3$ mode in the admixture gradually. That is why dipolar plasmon energy in finite field approaches $l = 1$ mode as the number of electrons increase.

The model we considered so far only accounted for the two-dimensional electron gas on a sphere where the electrons are delocalised and their wave function spreads out over the entire bubble but electrons on a spherical surface can also form a Wigner lattice where the electrons are localised.[22] The plasmons in the former case are the poles of the density-density correlation function whereas the plasmons in the latter case can be regarded as the phonons of the Wigner lattice.

We will now explore this second scenario. Klimin et. al. have recently derived a plasmon dispersion relation for an electron Wigner lattice in multielectron bubbles.[23] It is given by

$$\omega(l) = \sqrt{\frac{Ne^2}{m_e r_0^3} \frac{l(l+1)}{l + \epsilon(l+1)}}, \tag{25}$$

where ϵ represents the dielectric constant of the helium. Since these plasmon modes represent the oscillation of charge density for localized electrons, it is possible to regard this model a nanoshell with infinitesimal thickness from a theoretical point of view. Nanoshells consist of a thin gold or silver shell around a dielectric core.[24–27] The electronic and optical properties of metallic shell structures have been of interest in the context of atomic physics as well. A general semiclassical approach (SCA) was developed and applied to describe collective resonances in inner atomic shells of heavy atoms.[28, 29] For a spherical shell geometry with a step-function charge density, SCA predicts two collective oscillation modes for each component of angular momentum.[29] The energies of these plasmons are given by

$$\omega_{l\pm}^2 = \omega_s^2 [1 \pm \frac{1}{2l+1} \sqrt{1 + 4l(l+1)x^{2l+1}}] \tag{26}$$

where $\omega_s = \sqrt{\frac{2\pi e^2 n_0}{m_e}}$ is the surface plasmon energy and x is the aspect ratio defined as the ratio between the inner and outer radii of the metallic shell. n_0 represents the volume electron density here.

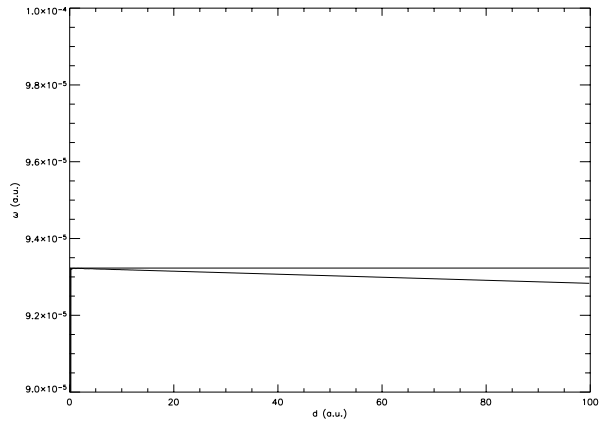

Figure 4. This figure illustrates the comparison between eq. (27) and eq. (25). X-axis shows d, thickness, in atomic units. The radius is 3980 a.u. and the number of electrons is 882. Straight line denotes the plasmon energy obtained from eq. (25) and the other line shows the plasmon energy obtained from eq. (27) for these parameters.

For a multielectron bubble in which the electron layer has a thickness on the order of a few nanometers, we can rewrite eq. (26) as

$$\omega_{l\pm}^2(\nu, d, r_0) = \frac{2\pi e^2 \nu}{d m_e}[1 \pm \frac{1}{2l+1}\sqrt{1 + 4l(l+1)(\frac{r_0 - d}{r_0})^{2l+1}}], \tag{27}$$

where d is the thickness of the electron layer and ν is the surface charge density. The relevant plasmon mode for this purpose in eq. (27) is ω_{l-} since the other one lies far higher in energy spectrum, thus it is very difficult to detect experimentally in most cases.

In fig. 4 we plotted eq. (25) and eq. (27) as a function of thickness of the electron layer and for $l = 1$. The radius is 3980 a.u. and the number of electrons is 882. We choose $\epsilon = 1$ in eq. (25) for the sake of simplicity so the plasmon energies obtained from these equations allow us to make a direct comparison between a 2D case and the 2D limit of a 3D case both of which are based on hydrodynamical models. It is clear from this figure that eq. (27) successfully recovers the result obtained from eq. (25) for infinitesimal thickness. This verifies our initial assumption that multielectron bubbles in Wigner lattice phase can be regarded as a nanoshell with infinitesimal thickness.

In reality, however, nanoshells are far thicker and much smaller than multielectron bubbles therefore, the present theoretical approach is not directly related to the the experimental data for nanoshells. Calculation of the electronic structure by using density functional theory which would take into account the effect of radial quantization and the magnetic field is required before one can obtain the optical structure. This case will be left for a future publication.

4. CONCLUSIONS

In this paper, we investigated the optical properties of a two-dimensional electron gas constrained on a spherical surface in the presence of a weak uniform magnetic field which causes Zeeman shift in electronic energy levels. We treated this problem perturbatively within the random-phase approximation scheme. We concentrated on the behaviour of the dipolar plasmon energy in particular. We found out that there is a blue-shift in this plasmon mode compared to its zero magnetic-field value and the shift tends to increase as a function of the magnetic field. We tried to understand in what conditions this perturbative approach is valid and when it starts failing.

We also analysed the behaviour of this plasmon mode as a function of the density of electrons on the sphere with and without the magnetic field. We showed that, in zero-field limit, this theoretical model fits perfectly to the semiclassical approach for a nanoshell of infinitesimal thickness. Further generalizations of this model for nanoshells of finite thickness are left for future studies.

ACKNOWLEDGMENTS

This work was supported by the Robert A. Welch foundation under the grant C-1222, by the Texas Advanced Technology Program, and by the Multi-University research Initiative of the Army Research Office. It is a pleasure to acknowledge valuable discussions with C. Dutta and computational help from C.Oubre. We are also very grateful to J. Tempere for his useful comments about the different phases of multielectron bubbles and Wigner crystallization.

REFERENCES

1. F. Haldane, "Fractional quantization of the hall effect: A hierarchy of incrompressible quantum fluid states," *Phys. Rev. Let.* **51 (7)**, pp. 605–608, 1983.
2. G. Fano, F. Ortolani, and E. Colombo, "Configuration interaction calculations on the fractional quantum hall effect," *Phys. Rev. B* **34 (4)**, pp. 2670–2680, 1986.
3. V.Melik-Alaverdian, N. Bonesteel, and G. Ortiz, "Quantum hall fluids on the haldane sphere: A diffusion monte carlo study," *Phys. Rev. Let.* **79 (26)**, pp. 5286–5289, 1997.
4. J. Yiang and W. Su, "A microscopic hierarchy theory of the fractional quantum hall effect," *J.Mod. Phys. B* **11 (6)**, pp. 707–728, 1997.
5. Y. Vlasov, V. Astratov, O. Karimov, A. Kaplyanskii, V.N.Bogomolov, and A.V.Prokofiev, "Existence of a photonic pseudogap for visible light in synthetic opals," *Phys. Rev. B* **55 (20)**, pp. R13357–R13360, 1997.
6. R. Averitt and N. Halas, "Plasmon resonance shifts of au-coated au_2s nanoshells: insight into multicomponent nanoparticle growth," *Phys. Rev. Lett.* **78 (22)**, pp. 4217–4220, 1997.
7. A. Volodin, M. Khaikin, and V. Edel'man, "Development of instability and bubblon production on a charged surface of liquid-helium," *JETP Lett.* **26 (10)**, pp. 543–546, 1977.
8. U. Albrecht and P. Leiderer, "Multielectron bubbles in liquid helium," *Europhys. Lett.* **3**, pp. 705–710, 1987.
9. H. Aoki and H.Suezawa, "Landau quantization of electrons on a sphere," *Phys. Rev. A* **46 (3)**, pp. R1163–R1167, 1992.
10. J. Kim, I.D.Vagner, and B. Sundaram, "Electrons confined on the surface of a sphere in a magnetic field," *Phys. Rev. B* **46 (15)**, pp. 9501–9504, 1992.
11. A. Ralko and T. Truong, "Heun functions and the energy spectrum of a charged particle on a sphere under a magnetic field and coulomb force," *J.Phys. A: Math. and General* **35**, pp. 9573–9583, 2002.
12. D. Bulaev, V. Geyler, and V. Margulis, "Magnetic response for an ellipsoid of revolution in a magnetic field," *Phys. Rev. B* **62 (17)**, pp. 11517–11526, 2000.
13. J. Rayleigh, "On the equilibrium of liquid conducting masses charged with electricity," *Phil. Mag* **14**, p. 184, 1882.
14. Y.Sasaki, Y. Nishina, M. Sato, and K. Okamura, "Optical-phonon states of sic small particles studied by raman scattering and infrared absorption," *Phys. Rev. B* **40 (3)**, pp. 1762–1772, 1989.
15. T. Inaoka, "Multipole excitations of an electron gas constrained to a spherical surface," *Surf. Sci.* **273**, pp. 191–204, 1992.
16. J. Tempere, I. Silvera, and J. Devreese, "Many-body properties of a spherical two-dimensional electron gas," *Phys. Rev. B* **65 (19)**, 2002.
17. D. Aristov, "Metallic nanosphere in a magnetic field: An exact solution," *Phys. Rev. B* **59 (9)**, pp. 6368–6372, 1999.
18. C.Flammer, *Spheroidal wave functions*, Stanford University Press, Stanford, 1957.
19. I. Komarov, L. Ponomarev, and S. Slavyanov, *Spheroidal and Coulomb spheroidal functions*, Nauka, Moscow, 1976.
20. J. Sakurai, *Modern quantum mechanics*, Addison-Wesley Co., New York, 1994.

21. A. Fetter and J.D.Walecka, *Quantum theory of many-particle systems*, McGraw-Hill, New York, 1971.
22. J. Tempere, S. Klimin, I. Silvera, and J. Devreese, "Wigner lattice of ripplopolarons in a multielectron bubble in helium," *Eur. Phys. J. B* **32**, pp. 329–338, 2003.
23. S. Klimin, V. Fomin, J. Tempere, I. Silvera, and J. Devreese, "Coupled ripplon-plasmon modes in a multielectron bubble," *Eur. Phys. J. B* **32**, pp. 329–338, 2003.
24. S. Oldenburg, R. Averitt, S. Westcott, and N. Halas, "Nanoengineering of optical resonances," *Chem. Phys. Lett.* **288**, pp. 243–247, 1998.
25. J. Jackson and N. Halas, "Silver nanoshells: variations in morphologies and optical properties," *J. Phys. Chem. B* **105 (14)**, pp. 2743–2746, 2001.
26. C. Graf and A. Blaaderen, "Metallodielectric colloidal core-shell particles for photonic applications," *Langmuir* **18 (2)**, pp. 524–534, 2002.
27. Y. Sun, B. Mayers, and Y. Xia, "Template-engaged replacement reaction: a one-step approach to the large-scale synthesis of metal nanostructures with hollow interiors," *Nano Lett.* **2 (5)**, pp. 481–485, 2002.
28. G. Mukhopadhyay and S. Lundqvist, "Collective motion in heavy atoms," *J. Phys. B: At. Mol. Opt. Phys.* **12 (8)**, pp. 1297–1304, 1979.
29. G. Mukhopadhyay and S. Lundqvist, "Density oscillations and density response in systems with nonuniform electron density," *Il Nuovo Cim. B* **27 (1)**, pp. 1–18, 1975.